Available online at www.sciencedirect.com

ScienceDirect

Mendeleev Commun., 2023, **33**, 380–383

Mendeleev Communications

Photoinduced recoordination in the complexes of bis-aza-18-crown-6-containing dibenzylidenecyclobutanone with alkali and alkaline-earth metal cations

Valery V. Volchkov,*[a] Mikhail N. Khimich,[a] Mikhail Ya. Melnikov,[a] Anton E. Egorov,[b] Roman O. Starostin,[a,c] Marina V. Fomina[c] and Sergey P. Gromov[a,c]

[a] *Department of Chemistry, M. V. Lomonosov Moscow State University, 119991 Moscow, Russian Federation. E-mail: volchkov_vv@mail.ru*

[b] *N. M. Emanuel Institute of Biochemical Physics, Russian Academy of Sciences, 119334 Moscow, Russian Federation*

[c] *Photochemistry Centre, FRC 'Crystallography and Photonics', Russian Academy of Sciences, 119421 Moscow, Russian Federation*

DOI: 10.1016/j.mencom.2023.04.026

Complexation with strong competitors (*i.e.*, Ba^{2+}, Ca^{2+}, and K^{+}) shortens the length of the chromophore in bis-aza-18-crown-6-containing dienones of 2,4-dibenzylenecyclobutanone series due to the weakening of π–LP conjugation as well as disruption of the quinonoid structure in the ground state of the dye (LP is the lone electron pair of the crown nitrogen atom). In the excited state, recoordination of metal cations in the crown cavity takes place. The complexation as well as the newly discovered photorecoordination in these metal complexes may be used to control the chromophore properties of the samples.

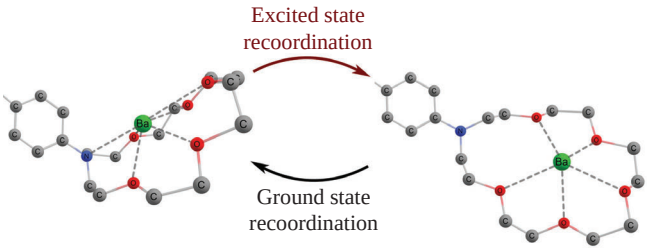

Keywords: bis-aza-18-crown-6-containing dienone, recoordination, alkali, alkaline-earth metal cation, supramolecular complex, TD DFT calculations.

Various donor–acceptor derivatives of mono- and bis-crown compounds with heteroatoms are often viewed as prototypes of photoswitchable molecular devices as well as optical, electrochemical, and colorimetric metal sensors. For instance, a hetarylazo chromophore covalently bounded to the mono-aza-18-crown-6 ether was proposed as a promising optical and electrochemical sensor for heavy metal cations (Hg^{2+}, Pb^{2+}).[1] 4-Acetylamino-1,8-naphthalimide derivatives containing an *N*-phenylazadithia-15-crown-5 were proposed as fluorescent chemosensors for Hg^{2+} cations in aqueous media.[2] The mechanism of color change involving an enol–ketone conversion of an azacrown dye modified with 4-(phenyldiazenyl)naphthalen-1-ol) was investigated as a colorimetrical sensor for Na^{+} cations.[3] Recently, a novel composite material based on polyvinyl chloride and a 1,8-naphthalimide derivative of azadithia-15-crown-5 was suggested as a selective highly sensitive fluorescent sensor for Ag^{+} cations in aqueous solutions.[4] The term 'adiabatic photorecoordination' (or 'decoordination') was introduced for the complexes of crown-containing styryl dyes (*i.e.*, optical sensors for alkali and alkaline-earth metal cations).[5,6] It should be noted that recoordination in crown compounds can be induced also by the thermal method.[7] Afterwards, the underlying nature of this process was deciphered *via* femto- and picosecond transient absorption spectroscopy of different crown compounds covalently bonded to the acceptor chromophore.[8–10] In general, recoordination involves three stages: first, the dissociation of the nitrogen–metal coordination bond; then, the cation shifting from its equilibrium position in the cavity; and finally, the metal being released into the solution. This process does not reach the final stage in every case, often stopping at the so-called 'loose' complex stage. Supposedly, photoejection into the solvent can only be detected when significant charge transfer takes place between the donor and the acceptor. Only in this case the nitrogen acquires a positive charge necessary for the electrostatic repulsion between the nitrogen atom and the metal cation that pushes the metal cation out of the crown cavity and into the solution. For example, intramolecular charge transfer in the 4-monoaza-15-crown-5-flavonol complex was hypothesized to be the main reason for metal ejection in MeCN.[11] The investigation of donor–acceptor complexes of the merocyanine DCM–azacrown with Ca^{2+} and Li^{+} cations confirmed photoinduced bond dissociation for the bonds between the coordinated metal cation and the nitrogen atom in the crown.[8–10] The red shift of the stimulated emission in the sub-picosecond time scale was specifically interpreted as pointing to the metal cation shifting within the crown cavity.[12] Depending on various cation–solvent or cation–counterion interactions, the recoordination may also depend on the conformation of the complex. Two stable conformations were found for the crowned lanthanide complexes of *N*-(2-salicylaldiminatobenzyl)-1-aza-18-crown-6.[13] In these cases, investigations may be complicated, requiring conformational analysis, selective excitation of individual complex types, *etc*. Since recoordination in the complexes of bis-azacrown ethers can involve disruption of one or two N–M bonds, correct interpretation of the experimental data can present additional difficulties. For example, the study of

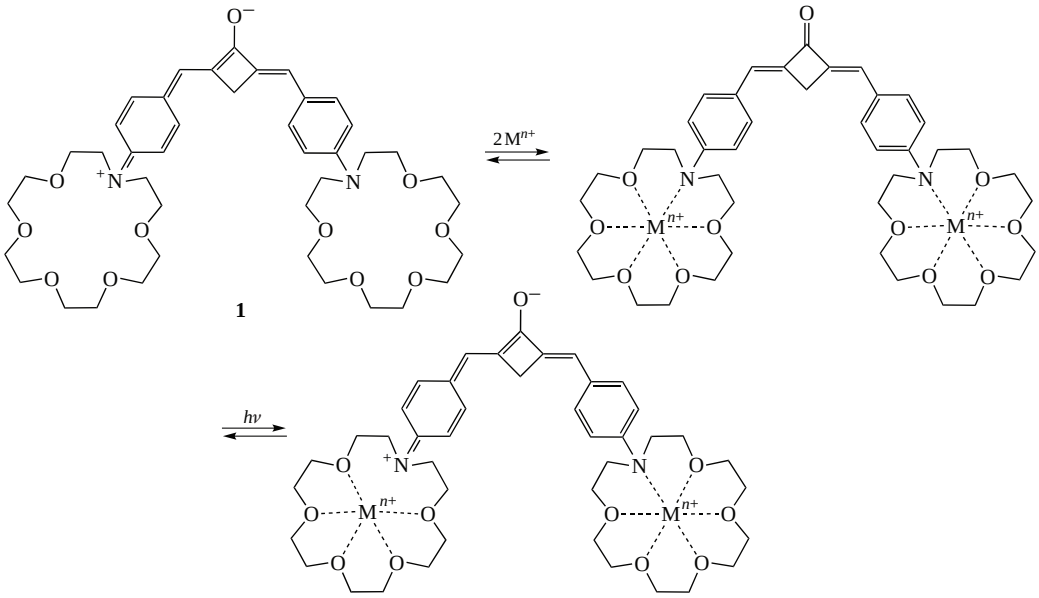

Scheme 1 Quinonoid form of dye **1**, complex **1**·$(M^{n+})_2$, (M^{n+} = Ba^{2+}, Ca^{2+}, K^+) in the ground and excited states (after recoordination).

a relatively symmetrical 2,5-{bis[4*N*-(aza-15-crown-5)phenyl]-methylene}cyclopentanone complex uncovered the formation of complexes of varying stoichiometry with metal perchlorates.[14,15] The spectral behavior of the excited calcium dicomplex (1 : 2) pointed to recoordination taking place with ejection of only one calcium cation into the solution.[16]

This paper constitutes the first part of our study of complex formation and photorecoordination in metal complexes of a novel bis-azacrown-containing compound with a cyclobutanone moiety in its center **1** (Scheme 1) being a fluoroionophore of the DAD type. The second part will include the analysis of femtosecond transient absorption data for dye **1** and several metal complexes. Rising interest in photoswitchable molecular receptors and devices for analytical application underscores the importance of this study. The details of spectral-luminescent measurements, calculations of stability constants as well as the limiting absorption spectra of 1 : 1 and 1 : 2 complex forms were published earlier.[17] The synthesis of compound **1** is beyond the scope of this study and will be published elsewhere. Calculation details, structural parameters of dyes and complexes as well as the purity confirmation of **1** with the corresponding ^{1}H HMR spectra (Figure S1) are presented in the Online Supplementary Materials.

The absorption spectrum of dienone **1** in MeCN is characterized by two bands: the intense long-wavelength band (λ_a^{max} = 477 nm) with a shoulder at 420 nm, arising from the $\pi \rightarrow \pi^*$ electronic transition with internal charge transfer from the crown moiety to the carbonyl group, and the less intense band (λ_a^{max} = 279 nm) arising from local $\pi \rightarrow \pi^*$ transitions. According to our calculations, the long-wavelength band corresponds to the HOMO → LUMO $\pi \rightarrow \pi^*$ transition (λ_a^{max} = 484 nm, f = 1.22), whereas its shoulder corresponds to the second HOMO-1 → LUMO $\pi \rightarrow \pi^*$ transition (λ_a^{max} = 419 nm, f = 0.23). The S_3 state refers to the forbidden HOMO-2 → LUMO $n \rightarrow \pi^*$ transition from the orbital localized on the carbonyl group (λ_a^{max} = 374 nm, $f \approx 0$). The absorption at 290 nm corresponds to local weak $\pi \rightarrow \pi^*$ transitions. The distribution of electronic density in dienone is shown in Figure S2 (see Online Supplementary Materials).

The complexation of **1** was studied *via* spectrophotometric titration in anhydrous MeCN using perchlorates of six different metals and trifluoroacetic acid. The isosbestic points in the absorption spectra could be observed in the following spectral series: **1**/MeCN/Ca^{2+} (439 nm), K^+ (440 nm), Li^+ (440 nm), and Mg^{2+} (441 nm). The spectral-thermodynamic parameters of the reaction are given in Table 1; the calculated absorption spectra for both types of complexes are shown in Figure 1. Generally, the reaction follows two stages described by equations (1) and (2). Conversion depends on the type of the metal involved.

$$M^{n+} \overset{K_s^{1:1}}{\longleftrightarrow} \mathbf{1}{\cdot}M^{n+} \quad (1)$$

$$\mathbf{1}{\cdot}M^{n+} + M^{n+} \overset{K_s^{1:2}}{\longleftrightarrow} \mathbf{1}{\cdot}(M^{n+})_2 \quad (2)$$

As inferred from the data in Table 1, the double-charged Ba^{2+} and Ca^{2+} cations are the most efficient complexing agents, yielding 1 : 1 and 1 : 2 forms with high stability constants. The large single-charged K^+ cations are characterized by lower values of stability constants. Smaller cations whose dimensions do not align with the dimensions of the 18-crown-6 cavity

Table 1 Absorption maxima (λ_a^{max}), extinction coefficients (ε_a^{max}), stability constants (logK_s) for **1**·M^{n+} (1 : 1) and **1**·$(M^{n+})_2$ (1 : 2) complexes, fluorescence maxima (λ_f^{max}) and fluorescence quantum yields (φ_f) in MeCN at 293 K, and cation diameters.[a]

Agent	λ_a^{max}/nm		ε_a^{max}/dm^3 mol^{-1} cm^{-1}		log[K_s (dm^3 mol^{-1})]		λ_f^{max}	φ_f	Cation diameter/Å
	1 : 1	1 : 2	1 : 1	1 : 2	1 : 1	1 : 2			
$Ca(ClO_4)_2$	466	442	42740	33580	5.88	4.05	606[b]	0.151[b]	1.98
$Ba(ClO_4)_2$	458	371	22520	42970	5.8	3.68	612[b]	0.169[b]	2.68
$Mg(ClO_4)_2$	464	–	39570	–	2.43	–	614[c]	0.08[c]	1.32
$LiClO_4$	469	–	47750	–	1.31	–	610[c]	0.15[c]	1.36
$NaClO_4$	473	–	48150	–	2.89	–	603[c]	0.163[c]	1.94
$KClO_4$	464	411	42280	37790	3.11	1.77	610[b]	0.085[b]	2.66
CF_3COOH	472	336	40500	41180	4.6	3.32	–	~0[b]	–

[a] ε_a^{max} (**1**) = 57600 dm^3 mol^{-1} cm^{-1}, λ_f^{max} (**1**) = 577 nm, φ_f (**1**) = 0.2. [b] For 1 : 2 complexes. [c] For 1 : 1 complexes.

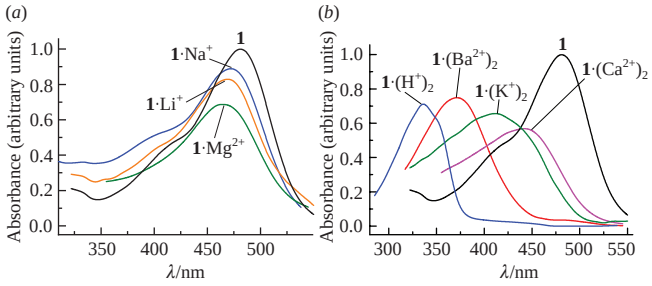

Figure 1 Calculated from spectrophotometric titration data for the long-wavelength absorption bands of 1 : 1 and 1 : 2 complexes of **1** with alkali, alkaline-earth metal cations, and trifluoroacetic acid in MeCN. Ratios of absorption intensities at spectral maxima are proportional to the ratios of corresponding extinction coefficients. The spectra of **1**·Ba^{2+}, **1**·Ca^{2+}, **1**·K^+, and **1**·H^+ forms are omitted for clarity.

(2.6–3.2 Å) mainly produce the 1 : 1 form with moderate stability constants. This behavior is typical for different bis-crown compounds with some variation depending on the nature of the central fragment in the fluorophore.[18,19] Generally, the stability constants vary with the charge and the dimensions of the cation, the crown size, the values of the partial negative charges on the oxygen/nitrogen heteroatoms in the crown as well as the conformations of the initial molecule and the resulting complexes.[20]

Since blue and red shifts in absorption and emission along with the Stokes shifts provide the measure of changes in the chromophore system upon complexation, they are the more informative parameters (Table 2). According to the results of our DFT calculations in the ground state for the related aza-crown containing styryl dye, there is a large population of the quinonoid form with pronounced π–LP conjugation between the side phenyl group and the lone pair of the neighboring nitrogen atom in the crown.[21] This explains the position of the long-wavelength absorption band. A similar calculation for dye **1** and its **1**·$(Ba^{2+})_2$ complex shows that the C–N and C–C bond lengths at the aryl fragment of the barium dicomplex exceed those for the initial dye in any of the calculated conformations (Table S3). This confirms a quinonoid form of **1** and the relevance of Scheme 1.

Upon complexation, the energy of long-wavelength electronic transitions increases to varying degrees. With weak competitors (such as Na^+, Mg^{2+}, and Li^+), weak blue shifts in absorption are observed (see Figure 1). Much stronger blue shifts arise for such strong competitors as K^+, Ca^{2+} and, especially, the large Ba^{2+} cation ($\Delta\nu_a$ = 5860 cm^{-1}). Notably, the long-wavelength absorption band of **1**·$(Ba^{2+})_2$ (λ_a^{max} = 371 nm) is shifted closer to the absorption band of (2*E*,5*E*)-2,5-dibenzylidenecyclopentanone, a closely related dye without two 18-crown-6 rings (**1′**, λ_a^{max} ~ 350 nm).[22] Correspondingly, the initial yellow-orange solution of **1** transforms into the colorless **1**·$(Ba^{2+})_2$ form. Additionally, when trifluoroacetic acid is used as the protonating agent for the crown nitrogen, complete discoloration of the solution is observed [for **1**·$(H^+)_2$, λ_a^{max} = 336 nm, see Figure 1; $\Delta\nu_a$ = 8930 cm^{-1}, Table 2]. This indicates either significant [for **1**·$(Ba^{2+})_2$] or complete [for **1**·$(H^+)_2$] disruption of the π–LP conjugation leading to the decay of the quinonoid form. Similar weakening of the π–LP conjugation was observed in other metal complexes [namely, **1**·$(Ca^{2+})_2$ and **1**·$(K^+)_2$], but to a lesser extent (see Figure 1). Apparently, these results point to the so-called 'axial type conformation' complexes, characterized by a metal–nitrogen bond and predicted for related supramolecular systems in MeCN.[23]

Structural parameters were calculated for the **1**·$(Ba^{2+})_2$ complex to confirm this assumption. We investigated the conformations of the complexes bearing 3, 4, and 5 molecules of MeCN for each metal cation with seven arrangement types for the solvent molecules, above and below the averaged plane of the crown molecule (3 : 0, 2 : 1, 4 : 0, 3 : 1, 2 : 2, 4 : 1, 3 : 2). The axial conformation of the **1**·$(Ba^{2+})_2$(ax), type 2 : 2 complex was found to be the most stable. Here, the amino group of the crown is significantly pyramidalized, and the C^6–N bond is longer than in the individual dienone molecule or its complex in the equatorial configuration [**1**·$(Ba^{2+})_2$(eq), see Table S1 and Figure S3 of Online Supplementary Materials]. The calculated absorption spectrum of the equatorial form resembles the spectrum of the individual dienone molecule, whereas the spectrum of the axial form resembles the experimental absorption spectrum of **1**·$(Ba^{2+})_2$. This supports our initial assumption.

Evidently, the $\Delta\nu_a$ values for the complexes with Ca^{2+} and K^+ indicate that the dimensions of the cation rather than its charge provide the most accurate factor of π–LP conjugation weakening. This may be explained by higher electrostatic attraction between the lone pair of the nitrogen atom and the K^+ cation at shorter distances. The absence of any long-wavelength shoulders in the long-wavelength absorption band at higher salt concentrations points to a single conformation (1 : 1 or 1 : 2) in the ground state.[23]

The red shifts in emission upon complexation are much smaller than the corresponding blue shifts in absorption (see Figure 2 and Table 2). This is typical for photoinduced recoordination of the metal cation in an excited complex with a broken metal–nitrogen bond. The cleavage of this bond upon excitation is the initial stage of recoordination.[24] Two additional processes take place: the restoration of the quinonoid conformation of the dye[7] and the shift for the metal cation within the crown cavity (see Scheme 1).[25] According to our calculations, upon excitation, the partial negative charges on the nitrogen atoms in the crowns become smaller due to the charges transferred to the central dienone acceptor (Table S2). Apparently, this phototransfer may be regarded as the main impetus behind recoordination.

The fluorescence quantum yields for each complex are somewhat lower than for the individual crown; the **1**·H^+ and **1**·$(H^+)_2$ forms are non-fluorescent. An anomalously large Stokes shift (10560 cm^{-1}) is observed for the **1**·$(Ba^{2+})_2$ complex. Usually, this is attributed to more pronounced changes in the

Table 2 Hypsochromic shifts in absorption ($\Delta\nu_a$), bathochromic shifts in fluorescence ($\Delta\nu_f$), Stokes shifts ($\Delta\nu_{a-f}$), fluorescence lifetimes (τ), and radiative and nonradiative rate constants of the **1**·M^{n+} (1 : 1) and **1**·$(M^{n+})_2$ (1 : 2) complexes in MeCN at 293 K.

Agent	$\Delta\nu_a$/cm^{-1}	$\Delta\nu_f$/ cm^{-1}	Stokes shift, $\Delta\nu_{a-f}$/cm^{-1}	$\tau^{a,b}$/ ns	$k_f \times 10^8$/ s^{-1}	$k_d \times 10^8$/ s^{-1}
$Ca(ClO_4)_2$	–580 (1 : 1) –1650 (1 : 2)	129 (1 : 2)	6170 (1 : 2)	1.53	0.99	5.55
$Ba(ClO_4)_2$	–880 (1 : 1) –5860 (1 : 2)	322 (1 : 2)	10560 (1 : 2)	1.55	1.09	5.36
$Mg(ClO_4)_2$	–675 (1 : 1)	412 (1 : 1)	5360 (1 : 1)	0.82	0.98	11.22
$LiClO_4$	–445 (1 : 1)	279 (1 : 1)	5060 (1 : 1)	1.21	1.24	7.02
$NaClO_4$	–265 (1 : 1)	~0 (1 : 1)	7880 (1 : 1)	1.09	1.5	7.67
$KClO_4$	–675 (1 : 1) –3454 (1 : 2)	220 (1 : 2)	8050 (1 : 2)	0.98	0.87	9.33
CF_3COOH	–353 (1 : 1) –8930 (1 : 2)	–	–	–	–	–

[a] Concentration of metal perchlorates in lifetime measurements: 1×10^{-3} M [$Ca(ClO_4)_2$ and $Ba(ClO_4)_2$], 1×10^{-1} M [$Mg(ClO_4)_2$], 2.75×10^{-1} M ($LiClO_4$), 3.5×10^{-1} M ($NaClO_4$), 1.19×10^{-2} M (saturated solution of $KClO_4$). [b] Measurement error <0.01 ns, τ(**1**) = 1.33 ns, k_f(**1**) = 1.5×10^8 s^{-1}, k_d(**1**) = 6.02×10^8 s^{-1}.

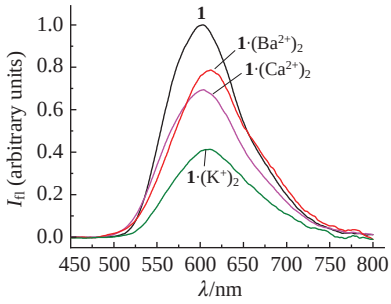

Figure 2 Quantum-corrected fluorescence spectra of dye **1** and the **1**·$(Ba^{2+})_2$, **1**·$(Ca^{2+})_2$, and **1**·$(K^+)_2$ complexes in MeCN at 293 K. The relative areas in the fluorescence spectra correspond to the ratios of the underlying φ_f values.

relaxed excited conformation of this complex in comparison with other complexes.

Fluorescence kinetics. The emission kinetics of **1** and the complexes are well-fitted by monoexponential plots. The highly stable **1**·$(Ba^{2+})_2$ and **1**·$(Ca^{2+})_2$ forms are characterized by somewhat longer lifetimes and lower k_d values than the others. Opposite behavior was detected for **1**·Mg^{2+}: approximately halved τ compared to the former values together with a twofold rise in the k_d value (see Table 2). The measured emission kinetics represent the conformations with already recoordinated metal cations: apparently, the recoordination does not reach its final stage, *i.e.* the ejection of the metal cation into the bulk solution (this is similar to the results for the crown-containing butadienyl dyes).[26] As mentioned before, only the axial form of the **1**·$(Ba^{2+})_2$ complex exists in the ground state since its excitation energy is larger than that for the equatorial form. Upon excitation, the axial form transforms into the equatorial configuration. Therefore, the metal cations within the crown cavity undergo recoordination.

The analysis of spectrophotometric and spectrofluorometric data together with the results of quantum-chemical calculations for the novel dienone dye **1** and its metal 1 : 1 and 1 : 2 complexes demonstrates the following. Partial quinonoid structure of the dye is disrupted in the course of complexation with alkali and alkaline-earth metal cations. Recoordination proceeds in the excited complexes with Ba^{2+}, Ca^{2+}, and K^+ cations. The so-called 'axial' conformation of the barium dicomplex with four molecules of MeCN and the more pyramidalized crown nitrogen is stable. Femtosecond time-resolved differential absorption spectroscopy is required to reveal the depth of the recoordination process in each individual case. The results obtained expand the possibilities of using bis-azacrown ethers showing supramolecular self-assembly and recoordination reaction for the development of photoswitchable supramolecular receptors and devices for analytical application.

This work was supported by the Russian Science Foundation (grant no. 22-23-00161). Synthesis of bis-aza-18-crown-6-containing dibenzylidenecyclobutanone was supported by the Russian Science Foundation (grant no. 22-23-00064). Quantum chemical calculations were carried out using the equipment of the shared research facilities of HPC computing resources at Lomonosov Moscow State University.

Online Supplementary Materials

Supplementary data associated with this article can be found in the online version at doi: 10.1016/j.mencom.2023.04.026.

References

1 P. Kaur, D. Sareen and K. Singh, *Dalton Trans.*, 2012, **41**, 8767.
2 P. A. Panchenko, A. S. Polyakova, Yu. V. Fedorov and O. A. Fedorova, *Russ. Chem. Bull.*, 2021, **70**, 1939.
3 L. M. Antonov, V. B. Kurteva, S. P. Simeonov, V. V. Deneva, A. Crochet and K. M. Fromm, *Tetrahedron*, 2010, **66**, 4292.
4 P. A. Panchenko, Yu. V. Fedorov, A. S. Polyakova and O. A. Fedorova, *Mendeleev Commun.*, 2021, **31**, 517.
5 S. P. Gromov, O. A. Fedorova, M. V. Alfimov, S. I. Druzhinin, M. V. Rusalov and B. M. Uzhinov, *Russ. Chem. Bull.*, 1995, **44**, 1922 (*Izv. Akad. Nauk, Ser. Khim.*, 1995, 2003).
6 S. I. Druzhinin, M. V. Rusalov, B. M. Uzhinov, M. V. Alfimov, S. P. Gromov and O. A. Fedorova, *Proc. Indian Acad. Sci., Chem. Sci.*, 1995, **107**, 721.
7 E. N. Ushakov, S. P. Gromov, O. A. Fedorova and M. V. Alfimov, *Russ. Chem. Bull.*, 1997, **46**, 484 (*Izv. Akad. Nauk, Ser. Khim.*, 1997, 463).
8 M. M. Martin, P. Plaza, N. D. Hung, Y. H. Meyer, J. Bourson and B. Valeur, *Chem. Phys. Lett.*, 1993, **202**, 425.
9 M. M. Martin, P. Plaza, Y. H. Meyer, F. Badaoui, J. Bourson, J. P. Lefevre and B. Valeur, *J. Phys. Chem.*, 1996, **100**, 6879.
10 P. Plaza, I. Leray, P. Changenet-Barret, M. M. Martin and B. Valeur, *ChemPhysChem*, 2002, **3**, 668.
11 A. Douhal, A. D. Roshal and J. A. Organero, *Chem. Phys. Lett.*, 2003, **381**, 519.
12 Ch. Ley, F. Lacombat, P. Plaza, M. M. Martin, I. Leray and B. Valeur, *ChemPhysChem*, 2009, **10**, 276.
13 M. González-Lorenzo, C. Platas-Iglesias, M. Mato-Iglesias, D. Esteban-Gómez, A. de Blas and T. Rodrıguez-Blas, *Polyhedron*, 2008, **27**, 1415.
14 A. O. Doroshenko, A. V. Grigorovich, E. A. Posokhov, V. G. Pivovarenko, A. P. Demchenko and A. D. Sheiko, *Russ. Chem. Bull.*, 2001, **50**, 404 (*Izv. Akad. Nauk, Ser. Khim.*, 2001, 386).
15 S. Fery-Forgues and F. Al-Ali, *J. Photochem. Photobiol., C*, 2004, **5**, 139.
16 N. Marcotte, P. Plaza, D. Lavabre, S. Fery-Forgues and M. M. Martin, *J. Phys. Chem. A*, 2003, **107**, 2394.
17 V. V. Volchkov, F. E. Gostev, I. V. Shelaev, V. A. Nadtochenko, S. N. Dmitrieva, S. P. Gromov, M. V. Alfimov and M. Ya. Melnikov, *J. Fluoresc.*, 2016, **26**, 585.
18 V. V. Volchkov, M. V. Rusalov, F. E. Gostev, V. A. Nadtochenko, A. I. Vedernikov, A. A. Efremova, L. G. Kuzmina, S. P. Gromov, M. V. Alfimov and M. V. Melnikov, *J. Phys. Org. Chem.*, 2018, **31**, e3759.
19 V. V. Volchkov, M. N. Khimich, M. V. Rusalov, F. E. Gostev, I. V. Shelaev, V. A. Nadtochenko, A. I. Vedernikov, S. P. Gromov, A. Ya. Freidzon, M. V. Alfimov and M. Ya. Melnikov, *Photochem. Photobiol. Sci.*, 2019, **18**, 232.
20 A. Ya. Freidzon, K. G. Vladimirova, A. A. Bagatur'yants, S. P. Gromov and M. V. Alfimov, *J. Mol. Struct.: THEOCHEM*, 2007, **809**, 61.
21 A. Ya. Freidzon, A. A. Bagatur'yants, S. P. Gromov and M. V. Alfimov, *Russ. Chem. Bull.*, 2008, **57**, 2045 (*Izv. Akad. Nauk, Ser. Khim.*, 2008, 2009).
22 M. V. Fomina, N. A. Kurchavov, A. Ya. Freidzon, V. N. Nuriev, A. I. Vedernikov, Yu. A. Strelenko and S. P. Gromov, *J. Photochem. Photobiol., A*, 2020, **402**, 112801.
23 A. Ya. Freidzon, A. A. Bagatur'yants, S. P. Gromov and M. V. Alfimov, *Russ. Chem. Bull.*, 2005, **54**, 2042 (*Izv. Akad. Nauk, Ser. Khim.*, 2005, 1981).
24 A. Ya. Freidzon, A. A. Bagatur'yants, S. P. Gromov and M. V. Alfimov, *Int. J. Quantum Chem.*, 2004, **100**, 617.
25 S. P. Gromov, S. A. Sergeev, S. I. Druzhinin, M. V. Rusalov, B. M. Uzhinov, L. G. Kuz'mina, A. V. Churakov, J. A. K. Howard and M. V. Alfimov, *Russ. Chem. Bull.*, 1999, **48**, 525 (*Izv. Akad. Nauk, Ser. Khim.*, 1999, 530).
26 M. V. Rusalov, B. M. Uzhinov, M. V. Alfimov and S. P. Gromov, *Russ. Chem. Bull.*, 2010, **59**, 1207 (*Izv. Akad. Nauk, Ser. Khim.*, 2010, 1182).

Received: 25th October 2022; Com. 22/7032